Article

Response and Mechanism of Coal Fine Production to Differential Fluid Action in the Baode Block, Ordos Basin

Boyang Wang [1], Yunfei Cui [1], Jingjing Li [1,*], Junjian Zhang [2], Longhui Bai [1] and Liu Wang [1]

[1] Key Laboratory of Continental Shale Hydrocarbon Accumulation and Efficient Development, Ministry of Education, Northeast Petroleum University, Daqing 163318, China; boyangwang@nepu.edu.cn (B.W.); 228002010058@stu.nepu.edu.cn (Y.C.); bailonghui0302@163.com (L.B.); wangliu@stu.nepu.edu.cn (L.W.)

[2] College of Earth Sciences & Engineering, Shandong University of Science and Technology, Qingdao 266590, China; junjianzhang@cumt.edu.cn

* Correspondence: lijingjing@cumt.edu.cn

Abstract: The Baode Block in the Ordos Basin is currently one of the most successfully developed and largest gas field of low–medium rank coal in China. However, the production of coal fine has affected the continuous and stable drainage and efficient development of this area. The special response and mechanism of differential fluid action during the drainage process is one of the scientific issues that must be faced to solve this production problem. In view of this, the evolution laws of a reservoir's macro–micro physical characteristics under different fluid conditions (fluid pressure, salinity) have been revealed, and the response mechanism of coal fine migration-induced reservoir damage has been elucidated through a nuclear magnetic resonance online displacement system. The results indicated that pores at different scales exhibited varying patterns with increasing displacement pressure. The proportion of the mesopore and transition pore is not affected by salinity and is positively correlated with displacement pressure. When the salinity is between 3000 mg/L and 8000 mg/L, the proportion of macropore and micropore showed parabolic changes with increasing displacement pressure, and there was a lowest point. The evolution law of pore fractal dimension and permeability change rate under the action of different fluids jointly showed that there was an optimal salinity for the strongest reservoir sensitivity enhancement effect. The mechanical and chemical effects of fluid together determined the damage degree of coal reservoir induced by coal fine migration.

Keywords: Baode Block; coal fine; fluid action; reservoir damage; fractal dimension

1. Introduction

Coal fine refers to the solid particles present, retained, or transported in reservoirs, pipelines, and drainage equipment systems during the development of coalbed methane (CBM) [1,2]. In view of the special mechanical properties of coal seams (low elastic modulus and high Poisson's ratio), the production of solid particles dominated by "coal fine" runs through the whole process of CBM development and is one of the key factors restricting CBM development [3]. How to solve the problem of reservoir damage caused by coal fine migration is a prerequisite for ensuring the efficient and stable drainage of CBM wells [4,5].

In the drainage stage, the coal fine and effective stress co-determine the change in reservoir permeability. The influence of coal fine migration on permeability has both advantages and disadvantages. If the fallen coal fine can be properly discharged, the seepage channel can be expanded, the permeability can be improved, and the gas production of a single well can be increased. On the other hand, when the detached coal fines are too large or the hydrodynamic conditions are insufficient to transport them, the precipitated coal fine will block the pores and fractures of the coal reservoir, leading to a decrease in permeability [6,7]. The impact of a large amount of coal fine production on the CBM drainage mainly includes the following aspects [8]: (1) reduced permeability, difficulty in

drainage and pressure reduction, and difficulty in gas desorption; (2) coal fine can cause wear on the pump barrel and plunger, causing problems such as buried pipe columns and pump jamming due to the accumulation of coal fine; and (3) the mixture of coal fine increases the fluid concentration and the construction pressure.

At present, the problem of coal fine production of medium–high ranking coal reservoirs (coal powder generation mechanism, migration mechanism, etc.) has been widely concerned by scholars at home and abroad [9–12], but research on the solid particles of low–medium rank coal reservoirs is relatively limited. The reasons for this are as follows: (1) the low rank coal in the Powder River Basin has extremely high reservoir permeability and shallow coal seam burial depth, often achieving high production without fracturing and other stimulation means, which significantly reduces the occurrence of coal fine production [13] and (2) the solid particles produced by low-rank coalbed methane wells (such as in the Surat Basin) are mainly inorganic minerals from sandstone and mudstone interlayers in coal measures, which is due to the thin interbedding of coal seams and sandstones in this basin, the low diagenesis of sandstones, and the easy disintegration into coal fine under the action of water sensitivity, acid sensitivity, etc. [14,15]. However, the physical properties and solid particle production of low–medium rank coal reservoirs in China are different from those in foreign countries, and the permeability is very low. Necessary measures such as fracturing to increase permeability will inevitably produce coal fine, which will affect the production of coalbed methane.

By analyzing the characteristics of coal fine produced in different drainage stages of CBM wells, it is believed that the amount of coal fine produced is controlled through the drainage management and control system and the characteristics of the reservoir, and the particle size of coal fine shows a significant downward trend with a longer period of drainage [16,17]. The particle size of coal fine is largest in the initial stage of drainage. If the settled coal fine blocks the coal reservoir, leading to a decrease in permeability, it will reduce the depressurization area of the coal seam and affect the subsequent drainage process. Therefore, studying the characteristics of coal fine production in the unidirectional flow stage is a prerequisite for developing a reasonable drainage system [18–20]. The physical simulation experiments of coal fine production are used to quantitatively characterize the characteristics of coal fine production under different geological conditions. Currently, quartz sand particles are mostly used to support coal bricks instead of raw coal or flat glass bead layers as seepage channels in order to study the impact of coal fine migration on the permeability of fractures. However, the impact of coal fine migration on pores is not yet known, especially for low–medium rank coal reservoirs mainly composed of matrix pore phases [21].

The intermediate bridge of the influence of coal fine migration on CBM production is the change in permeability, which is essentially the migration of solid particles and the blocking of the seepage channel, thus causing the possibility and degree of reservoir permeability decline [22,23]. Based on the physical simulation experiments of coal fine production via single-phase flow displacement, many scholars characterized the impact of coal fine production on reservoir damage by focusing on macroscopic changes in permeability [24–26]. However, micro-dynamic changes, such as pore structure and flow path, are often ignored when coal fines block the pore or fracture, resulting in an insufficient understanding of the micro-mechanism of coal fine migration-induced reservoir damage. Because pore structure is often the key to the critical conditions for particle separation, changes in the fluid migration channel can provide substantial evidence for particles blocking pores. Therefore, how to quantify/visualize the dynamic evolution characteristics of pore structure and fluid migration path during coal fine migration should be the next focus of research.

The proven geological reserves of coalbed methane in the Baode Block on the eastern edge of the Ordos Basin are 343.54×10^8 m^3, which is one of the most successful and large-scale low–medium rank CBM fields in China [27]. However, through the analysis of well production data, it was found a total of 492 drainage wells are affected by coal

fine, accounting for 51% of the whole area, thus affecting about 57,000 m^3 of daily gas production. The results of pump inspections over the years showed that the impact of coal fine leads to pump inspections being carried out on over 60 wells, accounting for over 10% of the total number of pump inspections (Figure 1). Coal fine production has significantly affected the development of coalbed methane in this research area [28]. The 8 + 9 coal is one of the main coal seams for the development of coalbed methane in the Baode Block, with an average thickness of 11.3 m and a gas content of 6.0–12.0 m^3/t. The reflectance of vitrinite ranges from 0.73% to 0.86%, belonging to low–medium rank coal. Based on this, No. 8 coal in the Baode Block of the eastern edge of the Ordos Basin was selected as the research object. With the help of an NMR (nuclear magnetic resonance) online displacement system, physical simulation experiments of coal powder production under conditions of variable fluid pressure and fluid salinity were carried out. Based on the variation law of reservoir permeability (macroscopic phenomenon), combined with the real-time observation of porosity, pore size distribution modification, and fluid migration during coal fine migration using NMRI (microscopic phenomenon), the quantitative characterization of reservoir damage was completed, and the response mechanism of coal fine migration induced reservoir damage under the coupling contract of coal fine–fluid–reservoir was revealed. The research results can not only provide a practical basis for the optimization of low–medium rank CBM development engineering designs and solve the problem of solid particle output but also promote and establish the evaluation methods and reservoir protection technology for China's low–medium rank coal reservoir protection effect and provide beneficial enlightenment for the large-scale and efficient development of low–medium rank CBM in China.
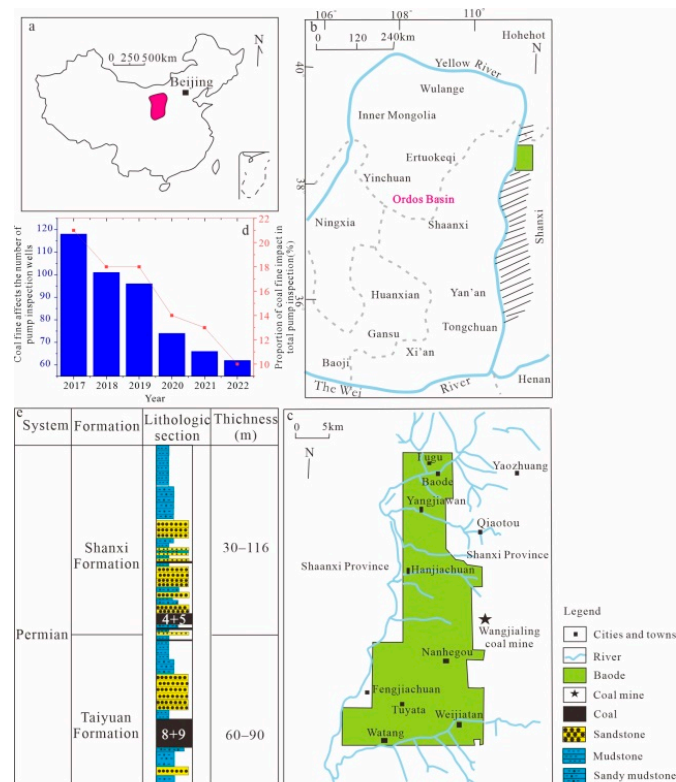

Figure 1. Geological location, coal stratigraphy, and coal fine influence ratio in the research area. (**a**) Location of the Ordos Basin (**b**) Location of the Baode block (**c**) Location of the scope of the Baode block (**d**) Coal fine impact the condition of pump inspection well (**e**) Stratigraphic synthesis histogram of the study area.

2. Geological Background

The Baode Block is located in the northern part of the eastern margin of the Ordos Basin. The main structure of the Baode Block is relatively simple. In general, it is a large monoclinal structure inclined to the NW with no developed faults and folds [29,30]. The groundwater in the study area mainly comes from atmospheric precipitation and the lateral recharge of Ordovician limestone, with runoff generally flowing from east to west. The coal-bearing strata in the area are mainly the Shanxi Formation and the Taiyuan Formation, followed by coal bearing sediments mainly composed of fluvial facies and delta facies and marine and continent interactive facies. The main coal seams for the development of CBM are the 4 + 5 coal seam of the Shanxi Formation (with an average thickness of 6.45 m) and the 8 + 9 coal seam of the Taiyuan Formation (with an average thickness of 9.16 m) [27]. The buried depth of the main coal seam is 300 m to 1200 m. The R_o is between 0.71% and 1.22%, which belongs to low–medium metamorphic bituminous coal. The gas content of the coal seam is 0 m^3/t to 12.0 m^3/t, the permeability is 0.2 mD to 10 mD, and the pressure coefficient is 0.65 MPa to 1.10 MPa, which is representative of underpressure or atmospheric reservoirs [31].

The development and exploration of coalbed methane in the Baode Block began in 2000 and has gone through four stages: foreign cooperation exploration evaluation stage (2000–2009), well group trial production evaluation stage (2010), integrated exploration and development pilot test stage (2011), and scale development and rolling expansion evaluation stage (2012 to present). At present, a total of 1100 wells have been drilled in the Baode Block, of which 960 are in production. By 2015, a production capacity of 5×10^8 m^3 has been built, and the production has been stable so far [27,31]. Through the analysis of well production data, a total of 492 drainage wells are affected by coal fine, accounting for 51% of the whole area, affecting about 57,000 m^3 of daily gas production. The results of the pump inspection over the years revealed that the impact of coal fine leads to pump inspections being carried out in over 60 wells, accounting for over 10% of the total number of pump inspections (Figure 1).

3. Samples and Methodology

3.1. Sample Basic Test

The primary structure coal of the 8 + 9 coal seam in Baode Block is selected as the research object. Five columnar coal samples (25 mm (diameter) × 50 mm (length)) were drilled from the same coal along the bedding direction via the wire cutting method for the physical simulation experiments of coal fine production. The sample at the end of the coal pillar was selected to basic testing. The maceral analysis and the maximum vitrinite reflectance measurements were performed following Chinese National Standards GB/T 8899-1998 [32] (the determination of maceral group composition and minerals in coal) and GB/T 6948-1998 [33] (the microscopical determination of the reflectance of vitrinite in coal). Proximate analysis was performed following Chinese National Standard GB/T 212-2001 [34] (the proximate analysis of coal). The porosity and permeability analysis was performed following Chinese petroleum industry standard SY/T 6385-2016 [35] (the porosity and permeability measurement under overburden pressure).

3.2. Physical Simulation Experiment of Coal Fine Production

The displacement fluid is configured in the laboratory based on formation water data, with the main cations being Ca^{2+}, Na^+, K^+, and Mg^{2+} and the main anions being Cl^- and HCO_3^-. Without considering the influence of external fluids, the average salinity of formation water is 3000 mg/L, with a maximum of 5000 mg/L [36]. When considering the influence of drilling or fracturing fluids, the average salinity of the fluid can reach 10,000 mg/L. Experimental injection fluids with different salinity levels were prepared, with five levels of 0 mg/L, 3000 mg/L, 5000 mg/L, 8000 mg/L, and 10,000 mg/L. The burial depth range of the 8 + 9 coal seam is 500 m to 1000 m [37]. Considering the average burial depth (800 m), the effective stress is set at 8 MPa. The experiments of coal fine production

under the action of differential fluid are essentially velocity sensitive experiments under different salinity degrees. Using the control variable method, a total of five experiments were conducted. The single velocity sensitive experiment adopts constant effective stress, gradually increasing injection pressure and confining pressure.

The experiment was carried out according to the Chinese petroleum industry standard SY/T5358-2010 [38] (formation damage evaluation via flow test). The experimental instrument was a nuclear magnetic resonance high-temperature and high-pressure displacement instrument (MesoMR23-060H-I). The instrument parameters are as follows: resonance frequency 23 MHz; magnet strength 0.3 T; coil diameters of 25 mm, 40 mm, and 60 mm; and a magnet temperature of 32 °C (Figure 2).
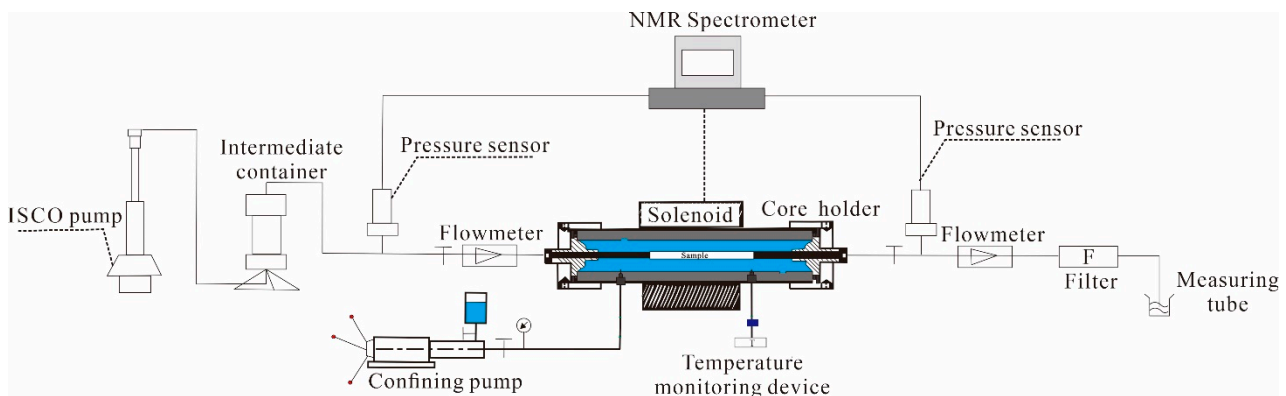

Figure 2. Structure diagram of NMR high-temperature and high-pressure displacement instrument.

The constant pressure method was used for testing, which involves the following: First, increase the displacement pressure through a displacement pump while increasing the confining pressure through an annular pressure pump to ensure that the effective stress remains constant during each displacement process. Gradually pressurize according to the prescribed displacement pressure and confining pressure, and measure in sequence until the difference between confining pressure and displacement pressure is 1.5 MPa. Close the displacement device and end the experiment (Tables 1 and 2). Collect the lateral relaxation spectrum and real-time image of the entire variable displacement pressure process, and measure the flow rate, pressure, time, etc., at specified time intervals. When the fluid state was almost stable, the experimental data were recorded, and each experimental datapoint was recorded three times. The average value was selected as the experimental test value to calculate the permeability change rate. Based on the above analysis, the dynamic quantitative characterization of the nuclear magnetic porosity, pore size distribution, and the permeability of the reservoir in the process of coal fine migration can be realized, and the visualization analysis of fluid migration can be realized in combination with real-time imaging. The CPMG parameters of this T_2 spectrum test sequence were as follows: P_1 = 5.52 μs, P_2 = 11.52 μs, SW = 200 KHz, RFD = 0.08 ms, RG1 = 20, DRG1 = 3, PRG = 0, TW = 3000 ms, TE = 0.1 ms, NECH = 6000, and NS = 16.

Table 1. Experimental scheme of physical simulation of velocity sensitive effect under different fluid conditions.

Sample Number	Salinity (mg/L)	Effective Stress (MPa)	Single Velocity Sensitive Experimental Conditions
BD-1-1	0	8	
BD-1-2	3000	8	
BD-1-3	5000	8	Table 2 for details
BD-1-4	8000	8	
BD-1-5	10,000	8	

Table 2. Design scheme of velocity sensitive experimental conditions under constant effective stress.

Injection Pressure (MPa)	Confining Pressure (MPa)	Effective Stress (MPa)	Single Displacement Time
1	8.5	8	
3	9.5	8	
5	10.5	8	Displace until the fluid state is nearly
7	11.5	8	stable and connect 500 mL of the
9	12.5	8	produced liquid with a measuring
11	13.5	8	cylinder.
13	14.5	8	

Note: The outlet pressure is atmospheric pressure, 0.1 MPa.

3.3. Data Processing Methods

(1) NMR pore size conversion combined with high-pressure mercury intrusion data

Firstly, nuclear magnetic calibration was conducted to establish the relationship between water volume and NMR intensity. The porosity of samples and the volume of saturated water were calculated. The results show that there was a significant positive correlation between water volume and NMR intensity (Figure 3).
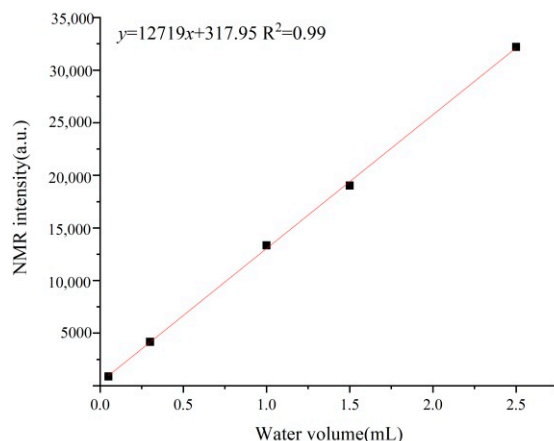
Figure 3. Relationship between water volume and NMR intensity.

Based on the high-pressure mercury intrusion data, compare and analyze NMR intensity with the nuclear magnetic T_2 spectrum and select a comprehensive relaxation rate (ρ) of 3 μM/s, which can then convert transverse relaxation time to the pore size. The specific process should correspond to Chinese National Standards GB/T 42035-2022 [39] (determination of pore size distribution of coal and rock using nuclear magnetic resonance). The pore structure is divided through a decimal aperture structure classification system. The statistics of a specific coal pore volume and the specific surface distribution of macropores (>1000 nm), mesopores (100~1000 nm), transition pores (10~100 nm), and micropores (<10 nm) were carried out.

(2) Fractal dimension calculation

NMR fractal theory was used to characterize reservoir pore heterogeneity under different fluid conditions [40,41], as shown in Formula (1).

$$\lg(V_P) = (3 - D_W)\lg(T_2) + (D_W - 3)\lg(T_{2\max}) \tag{1}$$

V_P is a cumulative spectral area percentage corresponding to different displacement pressure differences in a saturated fluid state, %; T_2 is the transverse relaxation time, ms; $T_{2\max}$ is maximum transverse relaxation time, ms; and D_W is the NMR fractal dimension value in a saturated water state.

Considering that the fractal curves of $\lg(V_P)$ and $\lg(T_2)$ have obvious inflection points, this suggests that the sample pores have multi-fractal characteristics. Combined with the

above pore size classification scheme, the fractal dimensions of micropores (D_1), transition pores (D_2), mesopores (D_3), and macropores (D_4) were obtained successively via piecewise fitting (Figure 4).
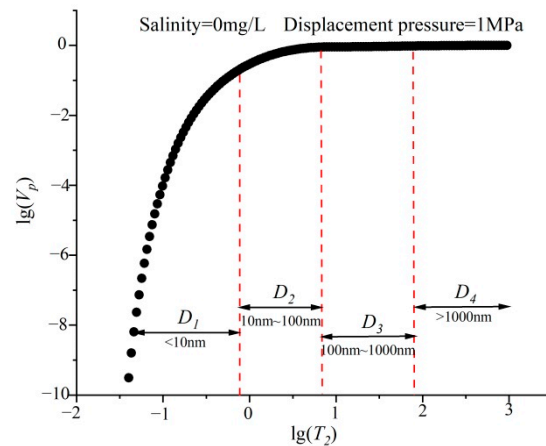

Figure 4. NMR fractal curves of samples with a salinity of 0 mg/L and a displacement pressure of 1 MPa.

4. Results and Discussion

4.1. Basic Characteristics of the Sample

The macrolithotype of the selected sample is semi-bright coal. The macerals are mainly composed of vitrinite, followed by inertinite, and the content of liptinite is the lowest. The inorganic components are mainly clay minerals, containing a small amount of carbonate and iron sulfide. The degree of thermal evolution belongs to low-metamorphic bituminous coal (Table 3).

Table 3. The basic information of the BD-1 coal sample.

Industry analysis and $R_{o,max}$ test	M_{ad} (%)	A_d (%)	V_{daf} (%)	FC_d (%)	R_o (%)
	1.98	9.65	35.59	59.62	0.68
Maceral with mineral matter	**Vitrinite (%)**	**Inertinite (%)**	**Liptinite (%)**	**Mineral matter (%)**	
	56.2	30.5	2.5	10.8	

Note: *M*, moisture; *A*, ash; *V*, volatile; *FC*, fixed carbon.

The porosity of the five samples ranges from 4.333% to 6.343%, with an average of 5.061%. The permeability ranges from 0.303 mD to 0.459 mD, with an average of 0.365 mD. The sample is mainly composed of transition pores, followed by micropores, with mesopores and macropores numbering the least. The pore size distribution of the displacement samples used under different salinity degrees is similar (Table 4, Figure 5).

Table 4. Porosity and permeability of samples.

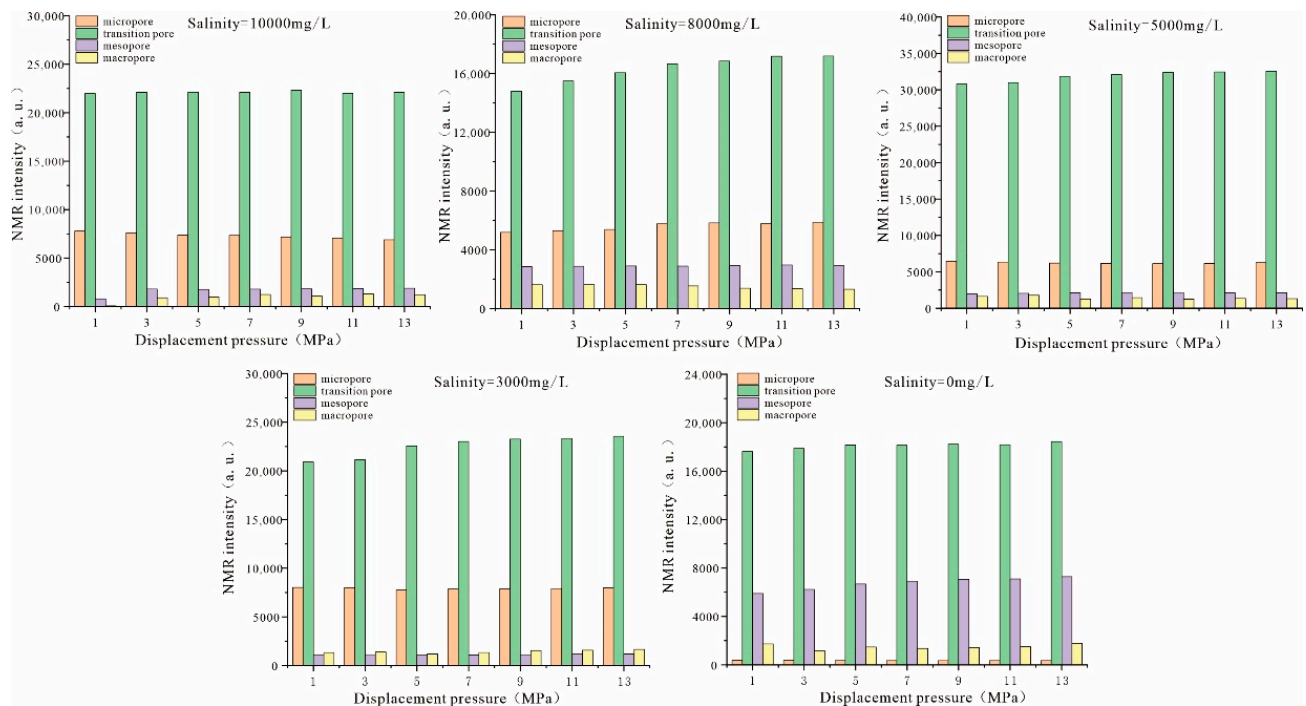| Sample Number	Length (cm)	Diameter (cm)	Porosity (%)	Permeability (mD)
BD-1-1	5.031	2.575	5.353	0.45929
BD-1-2	5.104	2.479	6.343	0.33752
BD-1-3	5.025	2.585	6.082	0.41539
BD-1-4	5.031	2.457	4.333	0.30313
BD-1-5	5.115	2.543	3.195	0.31189

Figure 5. Pore size distribution characteristics of samples under different salinity degrees and displacement pressures.

4.2. Changes in Macro–Micro Physical Properties of Coal Reservoirs under Different Fluid Conditions

When the salinity is 10,000 mg/L, with the gradual increase in displacement pressure, different scales of pores exhibit different variation characteristics. There is a significant positive correlation between micropores, transition pores, mesopores, and displacement pressure, while there is a significant negative correlation between macropores and displacement pressure (Figure 6). The porosity increases with the increase in displacement pressure, but there is a significant negatively correlating exponential relationship between permeability and displacement pressure (Figure 7). The above phenomenon indicates that the scour effect caused by an increase in flow velocity can lead to the generation and migration of secondary coal fines [42], which is the reason for the increase in micropores, transition pores, mesopores, and porosity. NMR imaging also verified the above conclusion. The area of the red part in the figure increased with the increase in displacement pressure, indicating that the pores of the sample increased, but the coverage area of the NMR signal decreased significantly, suggesting that the fluid migration channel gradually became smaller and that the fluid mainly flowed along the dominant channel (Figure 8).

When the salinity is 8000 mg/L, with the increase in displacement pressure, the micropores, mesopores, and macropores first decrease and then increase, while the transition pores showing a significant increasing trend (Figure 9). The porosity and permeability are also positively correlated with displacement pressure (Figure 10). Nuclear magnetic imaging also shows that both the red area and the nuclear magnetic signal area increase with the increase in displacement pressure (Figure 11).

When the salinity continues to decrease to 5000 mg/L, the variation trends of various pores are the same as when the salinity is 8000 mg/L (Figure 12). The porosity and permeability tend to increase with the increase in displacement pressure, but the increase amplitude is slightly lower than that when the salinity is 8000 mg/L (Figure 13). Magnetic imaging analysis also shows that with the increase in displacement pressure, the fluid seepage channel displays an increasing trend (Figure 14).
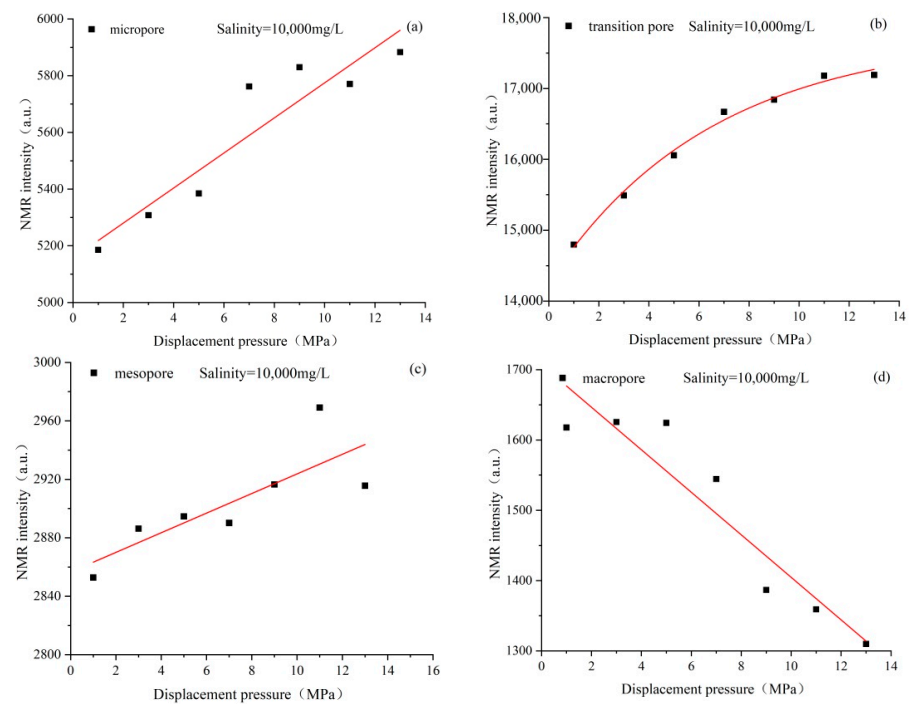
Figure 6. (**a**–**d**) Variation in pore size at different scales with displacement pressure under a salinity degree of 10,000 mg/L.
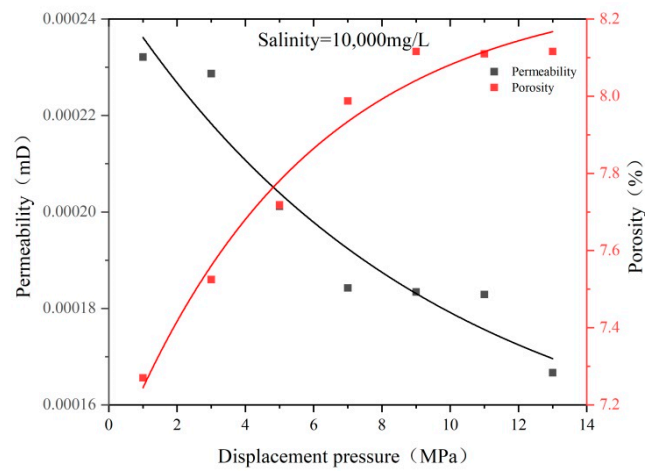

Figure 7. Permeability and porosity change with displacement pressure under a salinity degree of 10,000 mg/L.
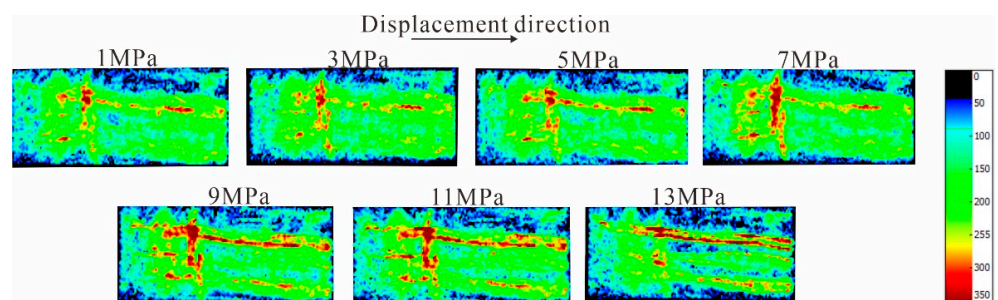

Figure 8. Nuclear magnetic imaging of longitudinal section of sample under a salinity degree of 10,000 mg/L.
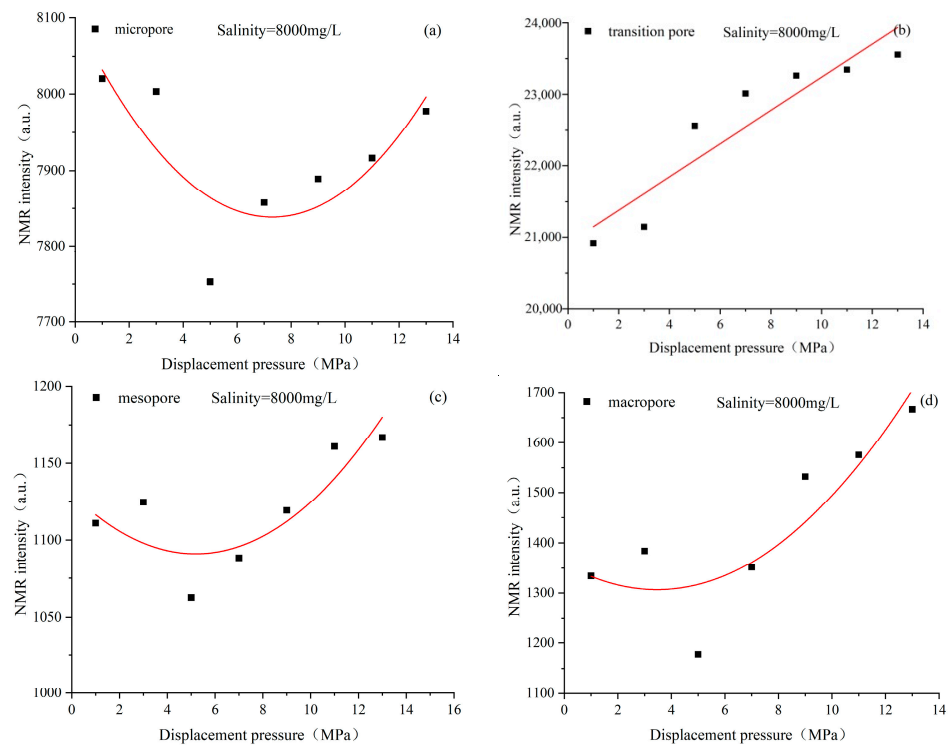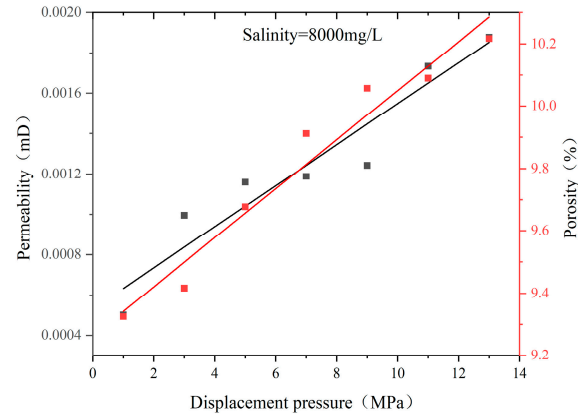
Figure 9. (**a–d**) Variation in pore size at different scales with displacement pressure under a salinity degree of 8000 mg/L.

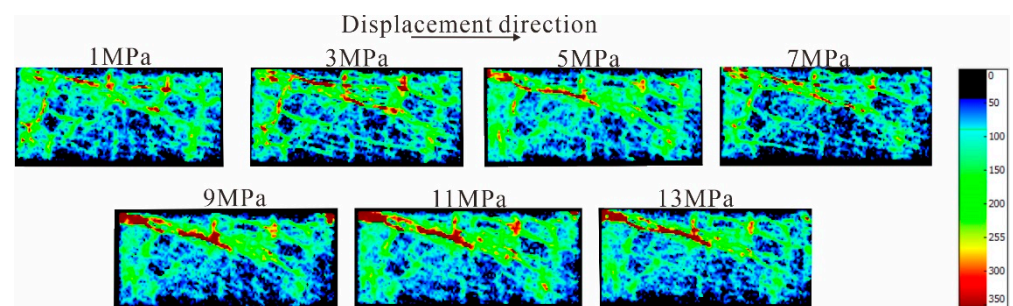**Figure 10.** Permeability and porosity change with displacement pressure under a salinity degree of 8000 mg/L.

Figure 11. Nuclear magnetic imaging of longitudinal section of sample under a salinity degree of 8000 mg/L.
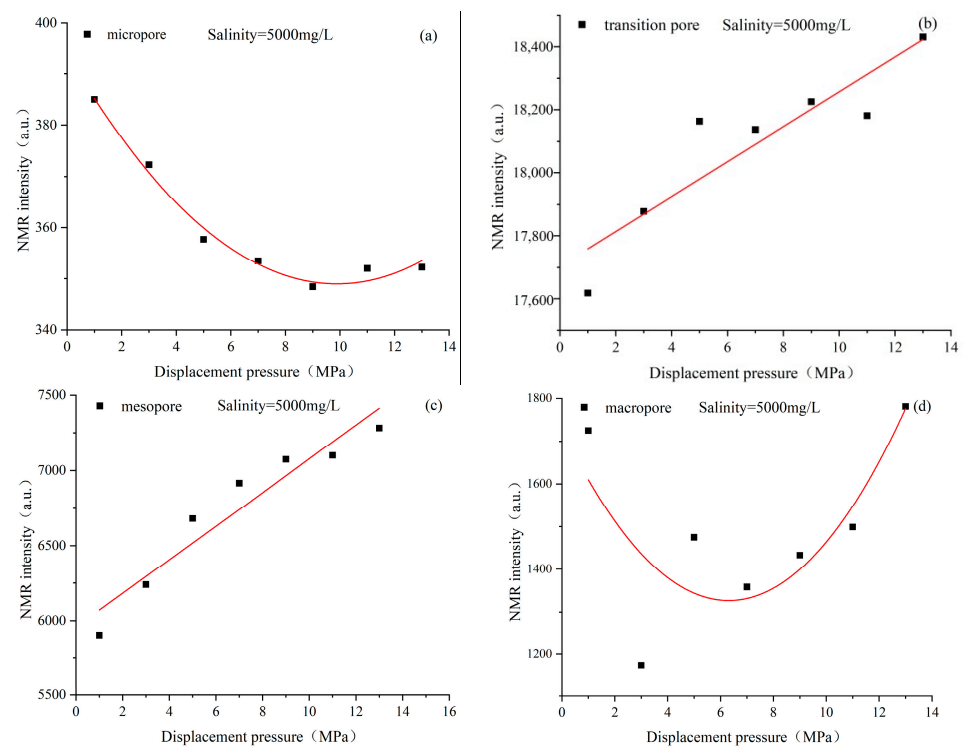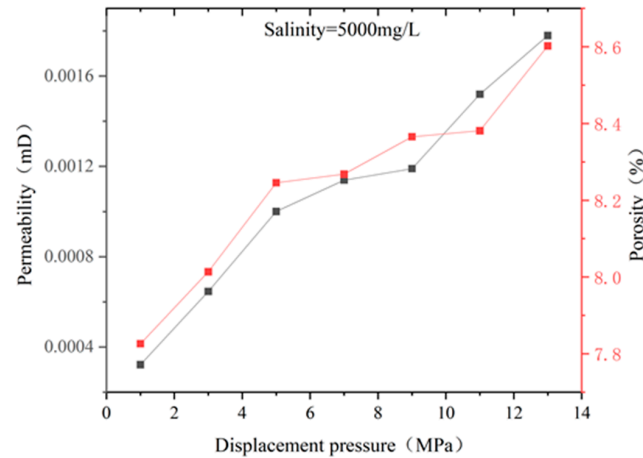
Figure 12. (**a**–**d**) Variation in pore size at different scales with displacement pressure under a salinity degree of 5000 mg/L.

Figure 13. Permeability and porosity change with displacement pressure under a salinity degree of 5000 mg/L.
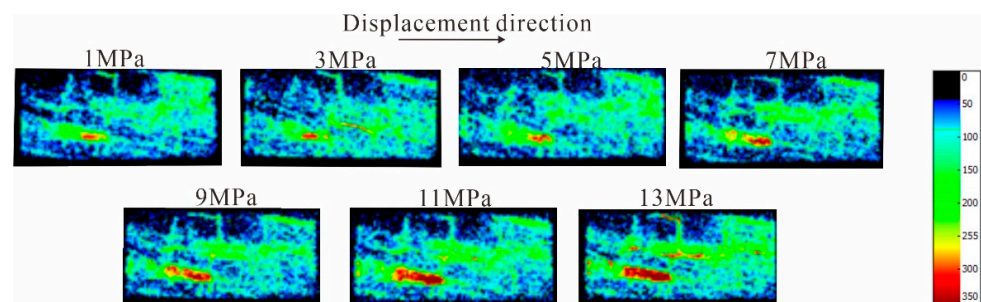

Figure 14. Nuclear magnetic imaging of longitudinal section of sample under a salinity degree of 5000 mg/L.

When the salinity continues to decrease to 3000 mg/L, along with the increase in displacement pressure, the transition pores and mesopores still show a significant increase trend, the micropores show a trend of first increasing and then decreasing, and the macropores show a negative correlation trend (Figure 15). The porosity increased slightly and the permeability decreased significantly with the increase in displacement pressure (Figure 16). This shows that the agglomeration of coal fine and the swelling of clay minerals together lead to the formation velocity sensitive effect. NMR imaging shows that with the increase in displacement pressure, there is no obvious dominant seepage channel, but only the local increase in NMR semaphore (Figure 17).
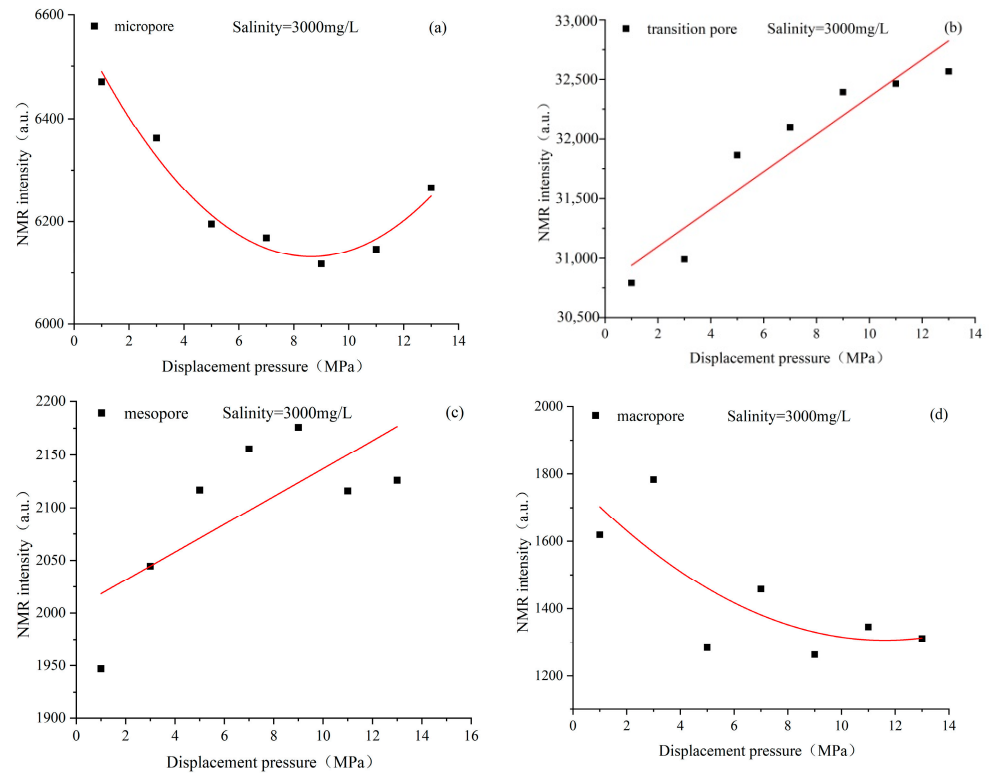
Figure 15. (**a**–**d**) Variation in pore size at different scales with displacement pressure under a salinity degree of 3000 mg/L.
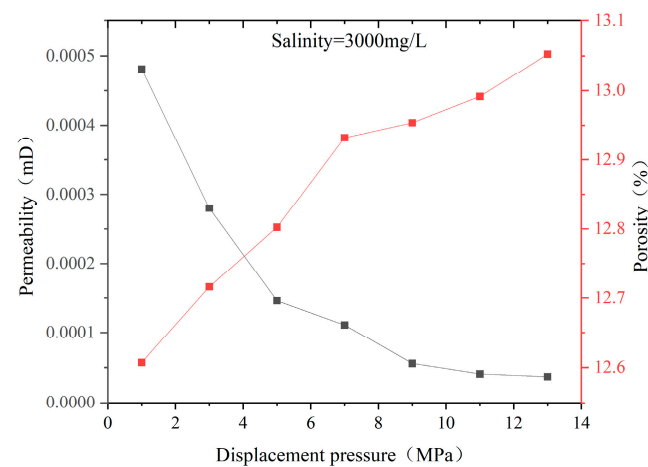
Figure 16. Permeability and porosity change with displacement pressure under a salinity degree of 3000 mg/L.
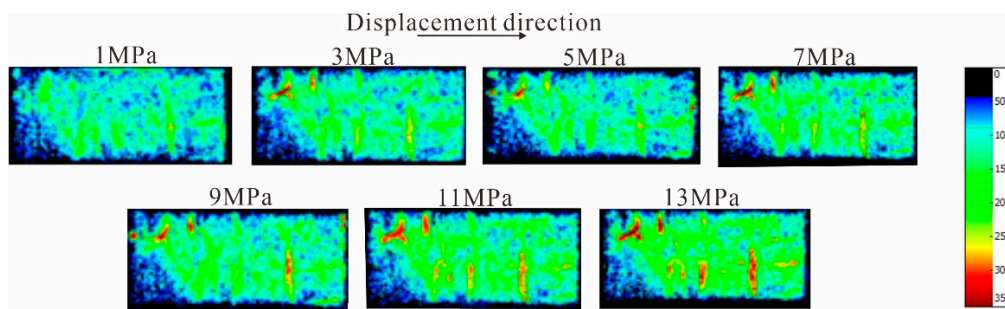
Figure 17. Nuclear magnetic imaging of longitudinal section of sample under a salinity degree of 3000 mg/L.

When the salinity decreases to 0 mg/L, the correlation between displacement pressure and pores of different scales become worse. From the analysis of NMR imaging and semaphore data, it can be seen that when the displacement pressure is 1 MPa, the NMR semaphore is low and the NMR imaging indicates that the saturated fluid in the core is too little, so this point is treated as an anomaly in this analysis (Figures 18–20).

With the increase in displacement pressure, only the micropores show a significant negative correlation, while the transitional pores show a weak positive correlation. The changes in mesopores and macropores are not significant with the increase in displacement pressure (Figure 18). This suggests that the agglomeration of coal fine and the hydration expansion of the clay mineral further aggravate the flow rate sensitivity of the reservoir, leading to a further reduction in permeability (Figures 18–20). The above conclusion is the same as that in Reference [43]. Under the conditions of NaHCO$_3$ solution displacement, the mass concentration of coal fine production decreases with the decrease in salinity degree. With the decrease in salinity degree, the negative charge on the surface of the coal fine is reduced via hydrolysis to produce OH$^-$, the repulsion between the coal fines is weakened, and the coal fine accumulation effect is significant. The decrease in reservoir permeability induced through the expansion of clay minerals caused by a reduction in salinity has been confirmed by many scholars [44–46].
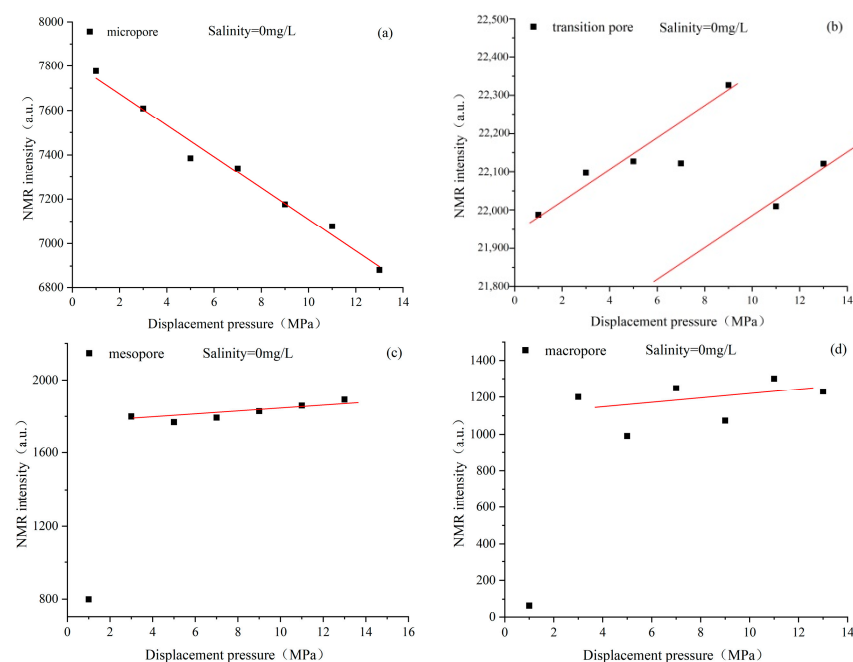

Figure 18. (**a–d**) Variation in pore size at different scales with displacement pressure under a salinity degree of 0 mg/L.
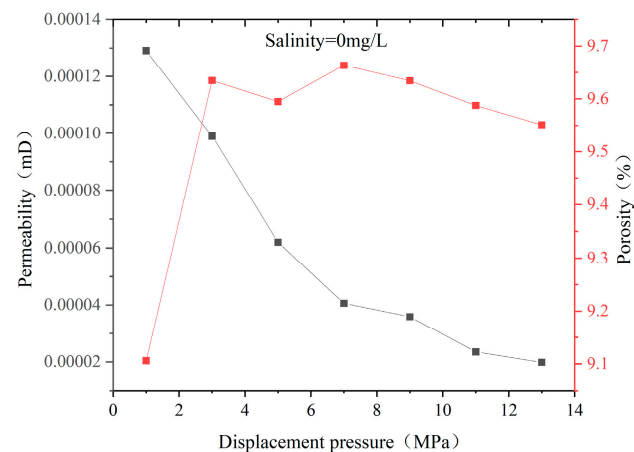
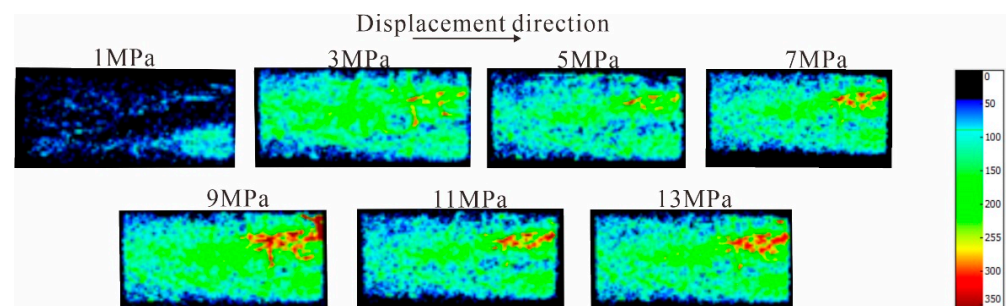**Figure 19.** Permeability and porosity change with displacement pressure under a salinity degree of 0 mg/L.

Figure 20. Nuclear magnetic imaging of longitudinal section of sample under a salinity degree of 0 mg/L.

4.3. Characteristics of Pore Structure Changes in Coal Reservoirs under Different Fluid Conditions

The results show that the fractal dimension values of micropores are all negative, which does not conform to the nuclear magnetic fractal definition, so it has no practical significance. The reason is that the adsorption force on the surface of the pore–fracture in the coal becomes the main force in the micropore stage, which binds the free flow of fluid and self-diffusion of fluid molecules. Therefore, both bulk relaxation and diffusion relaxation have important effects on the nuclear magnetic relaxation time and cannot be ignored. When the pore size and pore volume become larger, the adsorption pore will gradually transform into seepage pore, and the influence of surface adsorption force will weaken, and the influence on the free flow of fluid and the self-diffusion of fluid molecules will become smaller, so the influence of volume relaxation and diffusion relaxation on NMR relaxation time can be ignored [47].

Based on the previous analysis, it can be seen that under salinity conditions of 10,000 mg/L, with an increase in displacement pressure, the transition pores and mesopores show an increasing trend, while the macropores show a decreasing trend (Figure 6). According to the change in the fractal dimension at different stages, although the number of transition pore and mesopore increases, forces such as fluid shear often destroy the original pore structure, making it more complex. The generation of a large number of secondary coal fines leads to the blockage of macropores, so the pore structure also becomes worse, which is reflected in the fact that the fractal dimension increases with the increase in displacement pressure. The permeability of the sample shows a negative correlation with the increase in displacement pressure, exhibiting extremely strong velocity-sensitive damage (Figure 21).
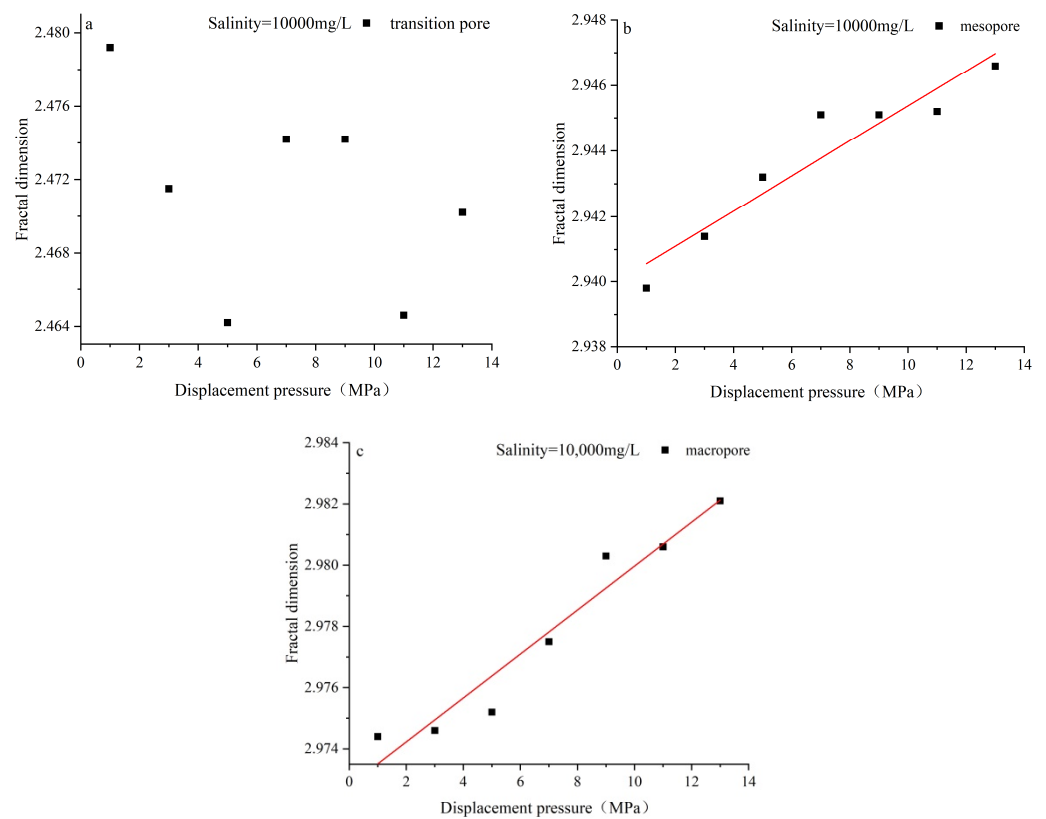
Figure 21. (**a**–**c**) Change in pore fractal dimension with displacement pressure under a salinity of 10,000 mg/L.

When the displacement pressure exceeds 5 MPa at a salinity of 8000 mg/L, the macropores, mesopores, and transition pores all increase with the increase in displacement pressure (Figure 9), and the fractal dimension of the various pore sizes mentioned above is negatively correlated with it. This indicates that the reduction in salinity increases the agglomeration effect of coal fines, and the particle size and quantity of coal fine suspension and transportation decrease, indirectly reducing the probability of coal fine clogging connected pores, thereby exhibiting a strong sensitization effect (Figure 22).

When the m salinity is 5000 mg/L, the critical displacement pressure difference increases to 7~9 MPa, and the macropores, mesopores, and transition pores increase with the increase in displacement pressure (Figure 12), and the pore fractal dimension is negatively correlated with it. It is shown that the increase in flow velocity after exceeding the critical flow velocity is beneficial for improving the seepage channel of the reservoir (the permeability increases with the increase in displacement pressure) (Figure 23). However, the agglomeration effect of coal fine is further increased due to the decrease in salinity, which leads to the weakening of the sensitization effect compared with the previous stage. In the low flow velocity stage (less than the critical displacement pressure), the accumulation of coal fine in the macropore leads to narrow seepage channels and complex pore structures.

With the further reduction in salinity, although the content of mesopores increases with the increase in displacement pressure, its fractal dimension is also positively correlated with the displacement pressure, indicating that the pore structure of mesopore tends to be complex. The macropore decreases with the increase in displacement pressure, and its fractal dimension is positively related to the displacement pressure, suggesting that its pore structure also tends to be complex. Generally speaking, the macropores and mesopores are seepage pores, so the sample permeability decreases with the increase in displacement pressure. For transition pores, although the pore content increases, the pore structure is negatively correlated with the increase in displacement pressure at the low displacement

pressure stage, but the transition pores are more inclined toward adsorption pores, so their influence on permeability is limited (Figure 24).
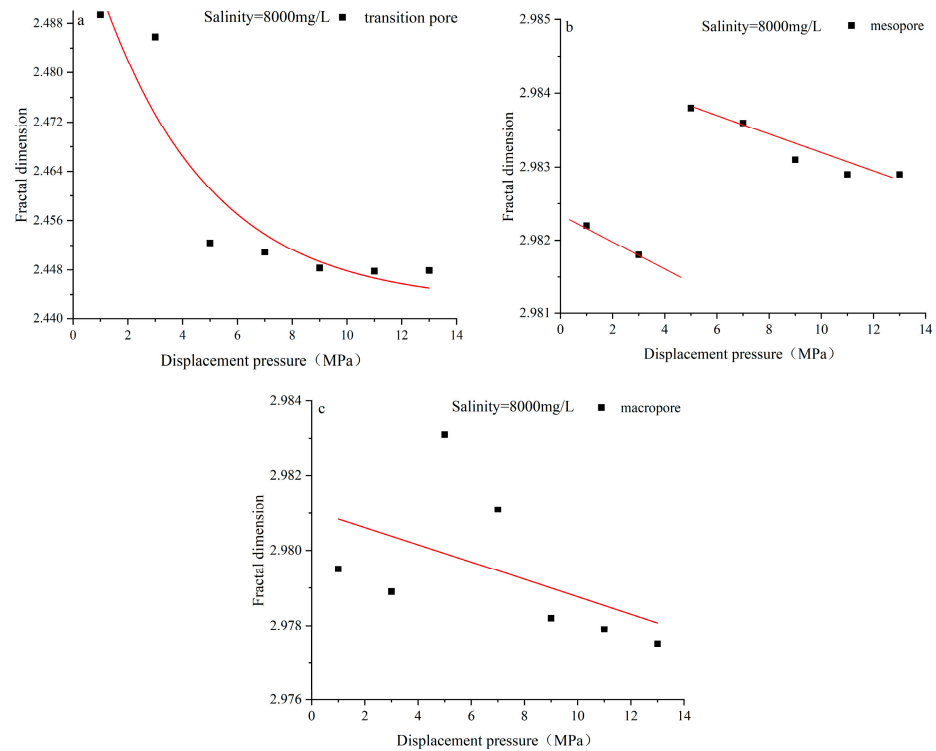

Figure 22. (**a–c**) Change in pore fractal dimension with displacement pressure under a salinity of 8000 mg/L.
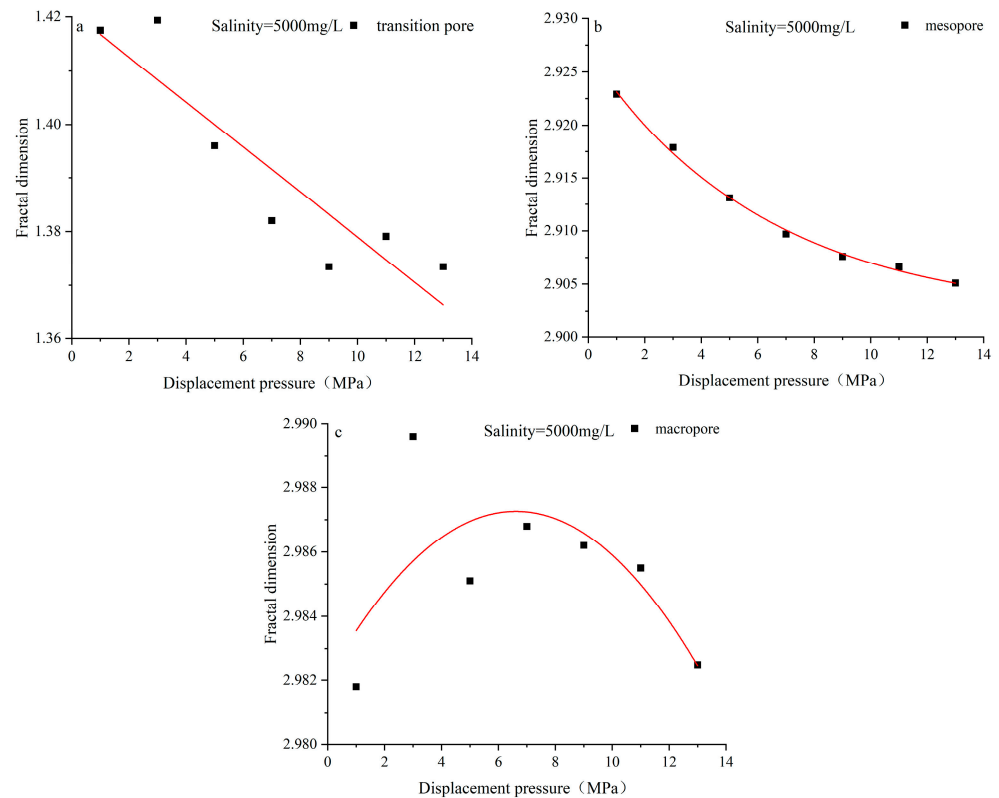

Figure 23. (**a–c**) Change in pore fractal dimension with displacement pressure under a salinity of 5000 mg/L.

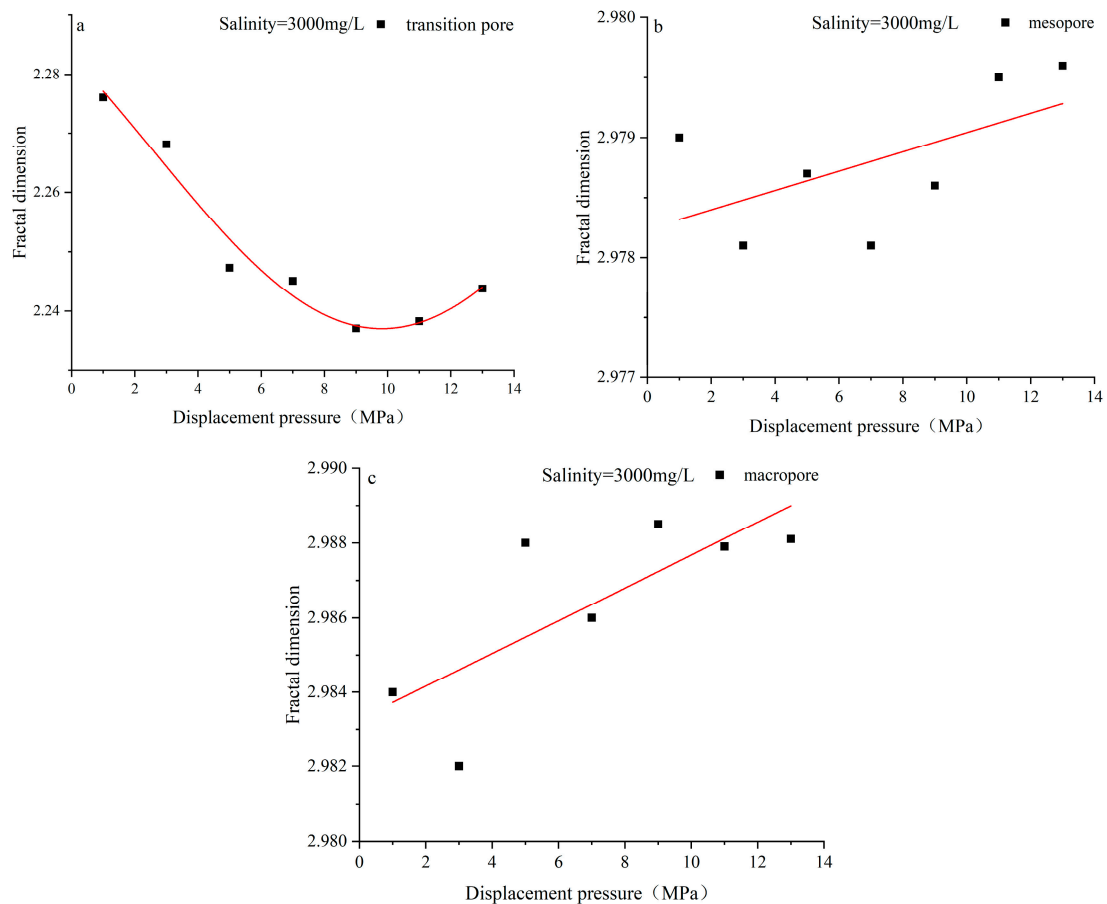**Figure 24.** (**a**–**c**) Change in pore fractal dimension with displacement pressure under a salinity of 3000 mg/L.

When the salinity is 0 mg/L, the pore fractal dimensions of different pore sizes are positively correlated with displacement pressure, indicating that the agglomeration of coal fine and the hydration expansion of clay minerals further aggravate the complexity of pore structure. The permeability is significantly negatively correlated with the increase in displacement pressure, suggesting that the reservoir velocity sensitivity is increased (Figure 25).

4.4. Response Mechanism of Coal Fine Migration-Induced Reservoir Damage under Different Fluid Action

In the process of CBM development, the injection of external fluids not only provides the fluid pressure that causes the generation and migration of coal fine but also induces changes in the mechanical properties of coal reservoirs (exacerbating coal fine production) and surface properties (affecting the flow state of coal fine) due to the reaction of fluids with different chemical properties with coal. Coal fine characteristics (particle size, composition, etc.), fluid characteristics, and reservoir pore–fracture space jointly determine the degree of reservoir damage caused by coal fine migration. How to accurately reveal the law of coal fine production and reservoir response mechanism in low–medium rank coal reservoirs under the action of different external fluids from the perspectives of mechanics and chemistry needs to be further examined [48,49].

The displacement under constant effective stress was adopted. The increase in displacement velocity and fluid pressure intensified the separation, start-up, and migration of coal fine. Based on the above analysis, it can be seen that under the experimental setting of salinity, the porosity, transition pore, and mesopore content of the coal reservoir increased with the increase in displacement pressure. The solid particles in the coal reservoir include

the original coal fine, the particles falling off due to hydrodynamic impact, and the particles expanding, dispersing, falling off, and participating in migration due to the hydration of clay mineral. Within the pore size range of 10~1000 nm, the fluid will carry solid particles in the coal reservoir fractures for migration. The higher the flow velocity rate, the more coal fine will be transported, resulting in an increase in porosity, transitional pore, and mesopore content.
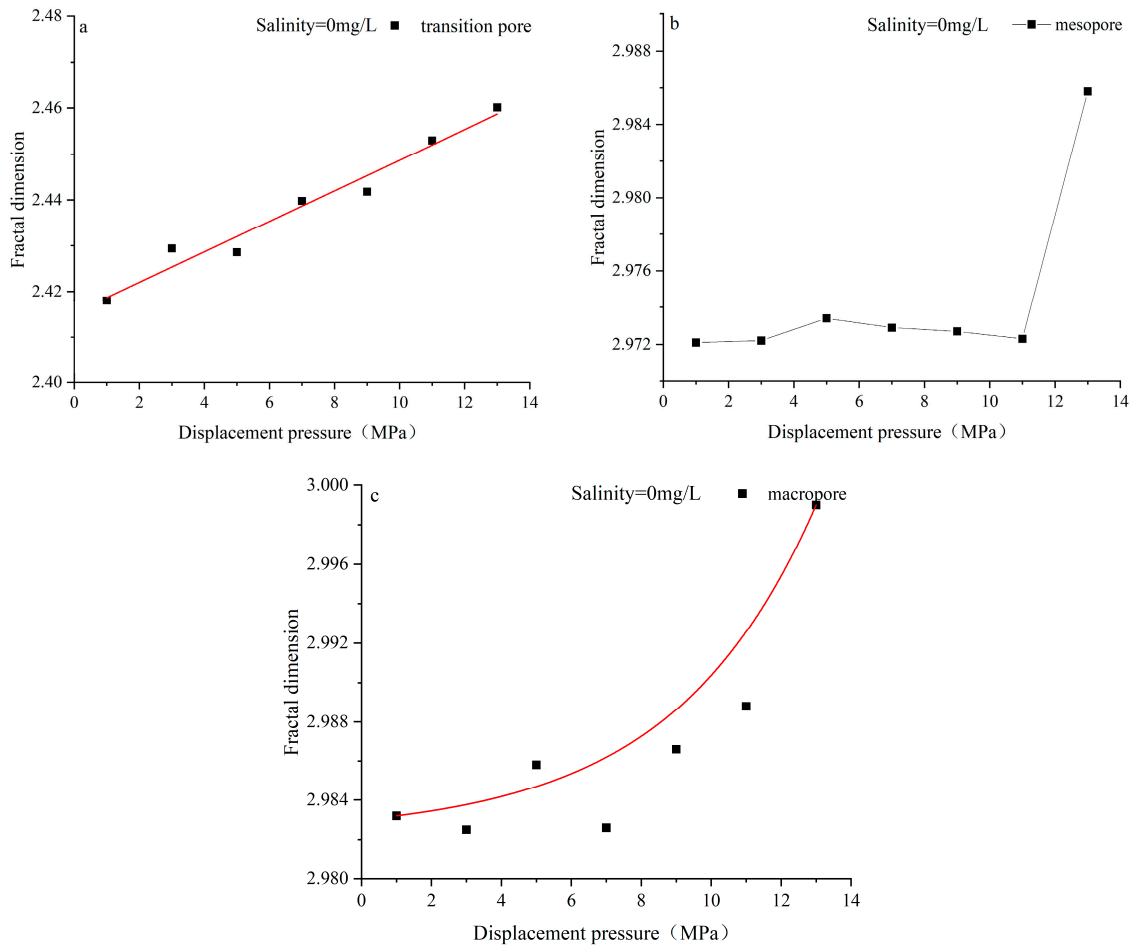
Figure 25. (**a–c**) Change in pore fractal dimension with displacement pressure under a salinity of 0 mg/L.

Regarding micropores, at lower salinity levels (0 mg/L), they mainly show a decreasing trend with the increase in flow rate. With the increase in salinity level (3000~8000 mg/L), they first decrease and then increase with the increase in flow velocity. When the salinity increases to 10,000 mg/L, they increase with the increase in flow velocity. For macropores, when the salinity is less than 3000 mg/L and the salinity is 10,000 mg/L, they show a decreasing trend with increasing flow rate. When the salinity is between 3000 mg/L and 8000 mg/L, it first decreases and then increases with increasing flow rate. The above phenomena indicate that hydrodynamic conditions are not the main controlling factor but are also affected by fluid chemistry. The chemical action of the fluid includes two main aspects. One is the impact of fluid chemical properties on the reservoir itself. For example, the water sensitivity of non-expansive clay particle migration induced by salinity change and the hydration expansion of clay mineral aggravate the generation of coal fine, which also leads to the increase in solid particles settling in micropores and macropores under low salinity, thus leading to the decrease in their content [50]. The second is the influence of fluid chemical properties on the surface properties of coal fine. The displacement fluid used in this study is $NaHCO_3$. Due to its weak acid radical in water, $NaHCO_3$ not only

ionizes but also undergoes hydrolysis reactions. With the increase in salinity, the anion OH⁻ generated by hydrolysis increases the surface negative charge of coal fine and enhances the repulsion force between coal fine particles. Coal fine is easy to disperse and not conducive to agglomeration [43]. Under the condition of high salinity, a large amount of coal fine is suspended, which also explains that with the increase in salinity, the decrease in water sensitivity and the weakening of agglomeration effects of coal fine, resulting in a more significant trend of increasing micropore content with the increase in flow velocity.

In order to evaluate the impact of coal fine migration on reservoir damage under different fluids, the rate of change (D_m) of permeability was calculated. The ratio of the difference between the permeability at a displacement pressure of 13 MPa and the permeability at a displacement pressure of 1 MPa to the maximum value of the two was used. When the salinity is less than 3000 mg/L, the change rate of the permeability is negative, and the fractal dimension of various pore sizes is significantly positive correlation with the increase in displacement pressure, indicating that the water sensitivity aggravates the pore heterogeneity, and the velocity sensitivity effect of the reservoir caused by coal fine migration increases. When the salinity is 10,000 mg/L, the permeability change rate is also negative, which indicates that there is also a strong velocity sensitive effect with the increase in flow rate. The main reason is that under the condition of high salinity, a large number of coal fines are suspended and migrated, which increases the probability of coal fines plugging the pore–fracture channels, so it is easy to have a very strong velocity sensitive effect, and the fractal dimension of various pore diameters is significantly positive correlation with the increase in displacement pressure. There is an optimal salinity range (5000~8000 mg/L), and the change rate of permeability is positive. With the increase in displacement pressure, the migration and output of coal fine can effectively improve the connectivity of reservoir. The fractal dimension of various pore sizes is significantly negatively correlated with the increase in displacement pressure (Figure 26). Liu et al. (2022) [43] also found that when NaHCO₃ is used as the displacement fluid, the permeability of the reservoir increases first and then decreases when the fluid salinity increases, which is consistent with the phenomenon obtained in this study. When the salinity degree is lower than the critical degree, the hydration expansion of clay minerals intensifies the production of coal fine [51], and the contact of low salinity degree water with coal fine changes their wettability and weakens the electrostatic force, leading to the migration of coal fine. Coal fine migration blocks the channel, increases the curvature of the fluid flow trajectory, and significantly reduces the permeability [52,53]. With the increase in salinity, the hydrolysis of NaHCO₃ leads to the increase in negative charge on the surface of coal fine, and the coal fine is easy to migrate, so the fluid has more space for distribution, which thus increases the permeability [54]. When the salinity degree continues to increase, a large amount of coal fine migration will form filter cakes [55] and will increase the probability of plugging pore–fracture channels, resulting in a decrease in permeability.
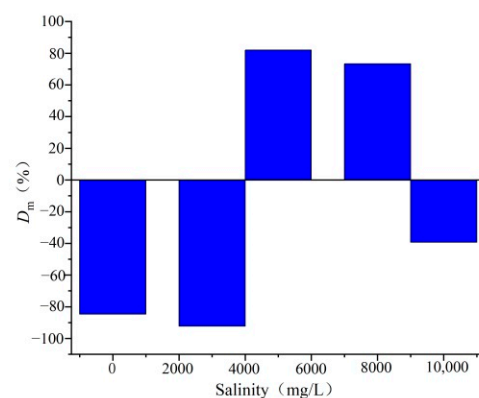

Figure 26. Change rate of permeability with salinity.

5. Conclusions

Under the conditions of experimental design salinity, the porosity, mesopores, and transitional pore content of coal reservoirs increase with the increase in displacement pressure. When the salinity is between 3000 mg/L and 8000 mg/L, the micropores and macropores decrease first and then increase with the increase in displacement pressure.

The permeability change rate and pore fractal dimension show the same change trend. That is, when the salinity is less than 3000 mg/L and more than 8000 mg/L, the permeability change rate is negative, and the fractal dimension of various pore diameters is positively correlated with the displacement pressure. When the salinity is between 3000 mg/L and 8000 mg/L, the permeability change rate is positive, and the fractal dimension of various pore diameters is significantly negatively correlated with the displacement pressure.

The water sensitivity of non-expansive clay particle migration induced by low salinity and the hydration expansion of clay minerals aggravates the generation of coal fine, and the water sensitivity aggravates pore heterogeneity, leading to the enhancement of the reservoir velocity sensitivity effect. The anionic OH^- generated through hydrolysis under high salinity conditions increases the negative charge on the surface of coal fine and enhances the repulsive force among coal fine particles. Coal fine is easy to disperse but not conducive to agglomeration. The suspension and transportation of a large amount of coal fine increases the probability of plugging the pore–fracture channels, so the reservoir velocity sensitivity effect is still strong. The existence of the optimal salinity (between 3000 mg/L and 8000 mg/L) causes the coal reservoir to have a strong sensitization effect.

References

1. Wei, Y.; Li, C.; Cao, D.; Zhang, A.; Yao, Z.; Xiong, X. The output mechanism and control measures of the pulverized coal in coalbed methane development. *Coal Geol. Explor.* **2018**, *46*, 68–73.
2. Awan, F.; Arif, M.; Iglauer, S.; Keshavarz, A. Coal fines migration: A holistic review of influencing factors. *Adv. Colloid Interface Sci.* **2022**, *301*, 102595. [CrossRef] [PubMed]
3. Wang, D.; Wang, Z.; Cai, X. Experimental study on coal fines migration and effects on conductivity of hydraulic fracture during entire coalbed methane production period. *Geoenergy Sci. Eng.* **2023**, *223*, 211555. [CrossRef]
4. Zhang, A.; Cao, D.; Wei, Y.; Rufford, T.E. Characterization of fines produced during drainage of coalbed methane reservoirs in the Linfen block, Ordos Basin. *Energy Explor. Exploit.* **2020**, *38*, 1664–1679. [CrossRef]
5. Chen, Y.; Ma, Z.; Ma, D.; Zhang, Z.; Li, W.; Yang, F.; Ji, Y.; Peng, T. Characteristics of the Coal Fines Produced from Low-Rank Coal Reservoirs and Their Wettability and Settleability in the Binchang Area, South Ordos Basin, China. *Geofluids* **2021**, *2021*, 5560634. [CrossRef]
6. Meng, Z.; Hou, Q. Experimental research on stress sensitivity of coal reservoir and its influencing factors. *J. China Coal Soc.* **2012**, *37*, 430–437.
7. Zhu, X.; Cao, D.; Wei, Y.; Yuan, Y.; Yao, Z.; Zhou, J.; Zhang, X. Study on Influencing Factors of Coal Fines Produced by CBM Wells in Hancheng block, Shaanxi Province, China. *Appl. Mech. Mater.* **2013**, *295–298*, 3228–3231. [CrossRef]
8. Chen, W.; Wang, S.; Qin, Y.; Zhao, W.; Zhao, J.; Yang, J.; Li, R. Migration and control of coal powder in CBM well. *J. China Coal Soc.* **2014**, *39*, 416–421.
9. Magill, D.; Ramurthy, M.; Jordan, R.; Nguyen, P. Controlling coal-fines production in massively cavitated openhole coalbed-methane wells. In Proceedings of the SPE Asia Pacific Oil & Gas Conference and Exhibition, Brisbane, QLD, Australia, 18–20 October 2010.
10. Massarotto, P.; Iyer, R.S.; Elma, M.; Nicholson, T. An experimental study on characterizing coal bed methane (CBM) fines production and migration of mineral matter in coal beds. *Energy Fuels* **2014**, *28*, 766–773. [CrossRef]

11. Guo, Z.; Vu, P.N.H.; Hussain, F. A laboratory study of the effect of creep and fines migration on coal permeability during single-phase flow. *Int. J. Coal Geol.* **2018**, *200*, 61–76. [CrossRef]

12. Awan, F.U.R.; Keshavarz, A.; Akhondzadeh, H.; Nosrati, A.; Al-Anssari, S.; Iglauer, S. Optimizing the dispersion of coal fines using sodium dodecyl benzene sulfonate. In Proceedings of the Asia Pacific Unconventional Resources Technology Conference, Brisbane, QLD, Australia, 18–19 November 2019.

13. Huang, P.; Kang, Y.; Deng, Z.; Li, G.; Mao, D.; Liu, H.; Zhao, Q.; Sun, T. Low coal rank coalbed methane accumulation model and exploration direction. *Acta Pet. Sin.* **2019**, *40*, 786–797.

14. Badalyan, A.; Beasley, T.; Nguyen, D.; Keshavarz, A.; Schacht, U.; Carageorgos, T.; You, Z.; Bedrikovetsky, P.; Hurter, S.; Troth, I. Laboratory and mathematical modelling of fines production from CSG interburden rocks. In Proceedings of the SPE Asia Pacific Oil & Gas Conference and Exhibition, Perth, Australia, 25–27 October 2016.

15. Ge, L.; Hamilton, C.; Ferbina, T.R.; Rudolph, V.; Rufford, T.E. Smart, porous polymer coatings to bind clay minerals in coal bed methane wells. In Proceedings of the International Petroleum Technology Conference, Bangkok, Thailand, 14–16 November 2016.

16. Wei, Y.; Li, C.; Cao, D.; Cui, B.; Xiang, X. Effect of pulverized coal dispersant on coal in the CBM well-washing technology. *J. China Coal Soc.* **2018**, *43*, 1951–1958.

17. Guo, Z.; Kang, N.; Le-Hussain, F. An NMR-assisted laboratory investigation of coal fines migration in fracture proppants during single-phase water production. *Fuel* **2023**, *343*, 127926. [CrossRef]

18. Zhao, X.; Liu, S.; Sang, S.; Pan, Z.; Zhao, W.; Yang, Y.; Hu, Q.; Yang, Y. Characteristics and generation mechanisms of coal fines in coalbed methane wells in the southern Qinshui Basin, China. *J. Nat. Gas Sci. Eng.* **2016**, *34*, 849–863. [CrossRef]

19. Zhong, Z.; Wu, X.; Han, G.; Li, C.; He, L.; Xiong, X.; Wang, S. Experimental investigation on particle transport of coal fines in unsteady terrain slug flow. *J. Pet. Sci. Eng.* **2018**, *166*, 747–758. [CrossRef]

20. Wei, Y.; Li, C.; Cao, D.; Zhang, A.; Wang, A.; Xiang, X. New Progress on the Coal Fines Affecting the Development of Coalbed Methane. *Acta Geol. Sin.-Engl.* **2018**, *92*, 2060–2062. [CrossRef]

21. Zou, Y.; Zhang, S.; Zhang, J. Experimental Method to Simulate Coal Fines Migration and Coal Fines Aggregation Prevention in the Hydraulic Fracture. *Transp. Porous Media* **2013**, *101*, 17–34. [CrossRef]

22. Bai, T.; Chen, Z.; Aminossadati, S.; Pan, Z.; Liu, J.; Li, L. Characterization of coal fines generation: A micro-scale investigation. *J. Nat. Gas Sci. Eng.* **2015**, *27*, 862–875. [CrossRef]

23. Shi, Q.; Qin, Y.; Zhou, B.; Zhang, M.; Wu, M.; Wang, L. An experimental study of the agglomeration of coal fines in suspensions: Inspiration for controlling fines in coal reservoirs. *Fuel* **2018**, *211*, 110–120. [CrossRef]

24. Bai, T.; Chen, Z.; Aminossadati, S.M.; Rufford, T.E.; Li, L. Experimental investigation on the impact of coal fines generation and migration on coal permeability. *J. Pet. Sci. Eng.* **2017**, *159*, 257–266. [CrossRef]

25. Huang, F.; Kang, Y.; You, Z.; You, L.; Xu, C. Critical conditions for massive fines detachment induced by single-phase flow in coalbed methane reservoirs: Modeling and experiments. *Energy Fuels* **2017**, *31*, 6782–6793. [CrossRef]

26. Hu, S.; Chen, Y.; Hao, Y.; Chen, Z.; Feng, G.; Li, G.; Guan, S.; Zhang, X.; Li, S. Experimental study of the effects of fine retention on fracturing proppant permeability in coalbed methane reservoirs. *J. Nat. Gas Sci. Eng.* **2020**, *83*, 103604. [CrossRef]

27. Xu, F.; Zhang, W.; Li, Z.; Zhang, L.; Zhang, J.; Hou, W.; Cheng, Q.; Li, Y.; Zhang, Q.; Hao, S.; et al. Coalbed methane reservoir description and enhanced recovery technologies in Baode block, Ordos Basin. *Nat. Gas Ind.* **2023**, *43*, 96–112.

28. Tao, S.; Tang, D.; Xu, H.; Li, S.; Geng, Y.; Zhao, J.; Wu, S.; Meng, Q.; Kou, X.; Yang, S.; et al. Fluid velocity sensitivity of coal reservoir and its effect on coalbed methane well productivity: A case of Baode Block, northeastern Ordos Basin, China. *J. Pet. Sci. Eng.* **2017**, *152*, 229–237. [CrossRef]

29. Liu, Y.; Li, S.; Tang, D.; Xu, H.; Tao, S.; Hu, X.; Zhu, X.; Ma, L. Mechanical behavior of low-rank bituminous coal under compression: An experimental and numerical study. *J. Nat. Gas Sci. Eng.* **2019**, *66*, 77–85. [CrossRef]

30. Chen, H.; Tian, W.; Chen, Z.; Zhang, Q.; Tao, S. Genesis of Coalbed Methane and Its Storage and Seepage Space in Baode Block, Eastern Ordos Basin. *Energies* **2022**, *15*, 81. [CrossRef]

31. Yang, X.; Mao, J.; Lin, W.; Hao, S.; Zhao, L.; Wang, Y.; Li, L. Exploration History and Enlightenment of Coalbed Methane in Baode Block. *Xinjiang Pet. Geol.* **2021**, *42*, 381–388.

32. *GB/T 8899-1998*; Determination of Maceral Group Composition and Minerals in Coal. Standards Press of China: Beijing, China, 1998; 8p. (In Chinese)

33. *GB/T 6948-1998*; Microscopical Determination of the Reflectance of Vitrinite in Coal. Standards Press of China: Beijing, China, 1998; 11p. (In Chinese)

34. *GB/T 212-2001*; Proximate Analysis of Coal. Standards Press of China: Beijing, China, 2001; 9p. (In Chinese)

35. *SY/T 6385-2016*; Porosity and Permeability Measurement under Overburden Pressure. Standards Press of China: Beijing, China, 2016; 9p. (In Chinese)

36. Yan, X.; Xiao, Z.; Wu, S.; Liu, Y.; Zhang, W.; Wang, Y.; Sun, X. Analysis of the Drainage and Production Effect of High Yield Water Wells in the Coalbed Methane Enrichment Area of Baode Block, Ordos Basin. *Nat. Gas Indus.* **2018**, *S1*, 86–93.

37. Yan, X.; Wen, S.; Nei, Z.; Sun, W. Re-recognition of geological factors affecting coalbed methane development effect. *Fault-Block Oil Gas Field* **2020**, *27*, 375–380.

38. *SY/T5358-2010*; Formation Damage Evaluation via Flow Test. Standards Press of China: Beijing, China, 2010; 32p. (In Chinese)

39. *GB/T 42035-2022*; Determination of Pore Size Distribution of Coal and Rock Using Nuclear Magnetic Resonance. Standards Press of China: Beijing, China, 2022; 13p. (In Chinese)

40. Qin, L.; Zhai, C.; Liu, S.; Xu, J.; Wu, S.; Dong, R. Fractal dimensions of low rank coal subjected to liquid nitrogen freeze-thaw based on nuclear magnetic resonance applied for coalbed methane recovery. *Powder Technol.* **2018**, *325*, 11–20. [CrossRef]

41. Zhao, Y.; Wang, C.; Ning, L.; Zhao, H.; Bi, J. Pore and fracture development in coal under stress conditions based on nuclear magnetic resonance and fractal theory. *Fuel* **2022**, *309*, 122112. [CrossRef]

42. Huang, F.; Dong, C.; You, Z.; Shang, X. Detachment of coal fines deposited in proppant packs induced by single-phase water flow: Theoretical and experimental analyses. *Int. J. Coal Geol.* **2021**, *239*, 103728. [CrossRef]

43. Liu, Z.; Wei, Y.; Zhang, Q.; Zhang, S.; Wang, A.; Cao, D. Physical simulation experiment of the effect of hydrochemical properties on the migration of coal fines in propped fractures. *J. China Coal Soc.* **2023**. [CrossRef]

44. Wang, B.; Qin, Y.; Shen, J.; Wang, G.; Zhang, Q.; Liu, M. Experimental study on water sensitivity and salt sensitivity of lignite reservoir under different pH. *J. Pet. Sci. Eng.* **2019**, *172*, 1202–1214. [CrossRef]

45. Wang, L.; Zhang, H.; Peng, X.; Wang, P.; Zhao, N.; Chu, S.; Wang, X.; Kong, L. Water-sensitive damage mechanism and the injection water source optimization of low permeability sandy conglomerate reservoirs. *Pet. Explor. Dev.* **2019**, *46*, 1218–1230. [CrossRef]

46. Shu, C.; Qu, R.; Li, Y.; Zheng, A.; Liu, T.; Dong, H.; Zhao, H.; Zhang, F.; She, Y.; Sun, S. Mechanism of microorganisms to relieve reservoir water sensitivity damage. *Pet. Sci. Technol.* **2023**. [CrossRef]

47. Hu, X.; Wang, C.; Sun, Q.; Dong, Z. Study on Fractal Characteristics of Pore Structure of Pyrolysis Coal by Nuclear Magnetic Resource Technology. *Min. Res. Dev.* **2021**, *41*, 67–75.

48. Han, G.; Ling, K.; Wu, H.; Gao, F.; Zhu, F.; Zhang, M. An experimental study of coal-fines migration in Coalbed-methane production wells. *J. Nat. Gas Sci. Eng.* **2015**, *26*, 1542–1548. [CrossRef]

49. Gao, D.; Liu, Y.; Wang, T.; Wang, D. Experimental Investigation of the Impact of Coal Fines Migration on Coal Core Water Flooding. *Sustainability* **2018**, *10*, 4102. [CrossRef]

50. Yao, Z.; Cao, D.; Wei, Y.; Li, X.; Wang, X.; Zhang, X. Experimental analysis on the effect of tectonically deformed coal types on fines generation characteristics. *J. Pet. Sci. Eng.* **2016**, *146*, 350–359. [CrossRef]

51. Chequer, L.; Vaz, A.; Bedrikovetsky, P. Injectivity decline during low-salinity water flooding due to fines migration. *J. Pet. Sci. Eng.* **2018**, *165*, 1054–1072. [CrossRef]

52. Yuan, B.; Moghanloo, R. Analytical model of well injectivity improvement using nanofluid preflush. *Fuel* **2017**, *202*, 380–394. [CrossRef]

53. Rosenbrand, E.; Haugwitz, C.; Jacobsen, P.; Kjoller, C.; Fabricius, I. The effect of hot water injection on sandstone permeability. *Geothermics* **2014**, *50*, 155–166. [CrossRef]

54. Wei, Y.; Zhang, J.; Wang, Y.; Cui, M.; Liu, Z.; Wang, A.; Cao, D. Experiment on the Effect of Water with Different Hydrochemistry on the Coal Fines Aggregation. *Coal Geol. China* **2023**, *35*, 1–8.

55. Keshavarz, A.; Yang, Y.; Badalyan, A.; Johnson, R.; Bedrikovetsky, P. Laboratory-based mathematical modelling of graded proppant injection in CBM reservoirs. *Int. J. Coal Geol.* **2014**, *136*, 1–16. [CrossRef]